P-12

CONSTRUCTING AN EFFICIENT CLASSIFIER MODEL FOR NATURAL VEGETATION USING REGIONAL CONVOLUTIONAL NEURAL NETWORKS

R.VIDHU[*], Dr.S.NIRAIMATHI[#]

Research Scholar in PhD, NGM College Pollachi.

[#]Associate Professor in PG Department of Computer Applications, NGM College, Pollachi.

***rvidhu24@gmail.com, [#]niraisenthil@hotmail.com.**

ABSTRACT

The computation of natural vegetation is a time-consuming and carried out monotonous. This work concentrates on providing a sensor-based natural vegetation process or monitoring system. The significant element for this vegetation process is based on IoT sensors with micro-controllers for system processing, establishing communications among the interconnected nodes and various connected sensors. Some real-time data access is performed with the remote monitoring technologies. An available online dataset is considered for validation using Regional- Convolutional Neural Networks (R-CNN) and a rule-based system model. This approach is used for analyzing the standardized values. When the collected values are higher than the fixed threshold value, an alert is generated and moved to the remote location. The efficiency of the proposed R-CNN model is used to acquire natural vegetation monitoring system with lower power devices, higher mobility, and precision values.The sensitivity of R-CNN model is 98.58%, 94.50% specificity, 98.89% PPV, 96.58% NPV, and 96.58% prediction accuracy.

Keywords: IoT- Internet of Things, regional convolutional neural networks,rule generation, higher mobility.

1. INTRODUCTION

It is noted that the forest inventory relies on the remote sensing approaches and forest management [1]. In remote sensing, light detection and ranging are adopted for accurately predicting the forest attributes, i.e., diameter and height of the tree, crown base height, leaf area index, and canopy cover for extracting more information. At present, Unmanned Aerial Vehicle (UAV)-borne, airborne, terrestrial LiDAR, and mobile are some of the commonly used approaches in the natural vegetation process. Moreover, these systems have their drawbacks in predicting the essential information [2]. The UAV-borne and down-looking airborne can offer highly resourceful canopy tree information; however, it lacks track information[3]. As this method, the mobile LiDAR system, i.e., the backpack, can offer essential tree truck information but lacks in providing the vertical field of measurement and view range and outcomes in the missed canopy information [4]. The terrestrial laser scanning-based single

location scans suffer from the occlusion effect over the leaves and trees and multi-scan TLS data registration, which is time-consuming [5]. The multi-platform data fusion has the efficiency to offer a resourceful solution to deal with the constraints of every detection and ranging platform.

At present, there are diverse commonly adopted cloud registration frameworks like point-based, feature-based, and target-based techniques [6]. Here, target-based approaches require the help of exterior data to registered detection and ranging point clouds, for example, positioning information from Global Positioning System (GPS), target registration can be predicted easily or color information attained from cameras. Next, feature-based approaches work like of target-based approach that uses polygons/lines/points for registering LiDAR points; however, these features are predicted with issues like traffic signs, roads, roofs, and buildings [7]. Subsequently, point-based approaches match directly with point clouds relying on the geometric information offered by these ranging points. The iterative nearest point approach is extensively adopted under these categories. Moreover, point cloud registration models are generally problematic over forest regions. The external registration information needed by the target-based methods is inaccurate, unavailable, or hard to attain in forests. For instance, GPS positioning data are unreliable over the forest canopies due to multi-path errors and GPS signal attenuation 8. Moreover, handling the ground targets or attaining color imagery is extremely expensive and time-consuming. Feature-based approaches are extensively utilized in urban and indoor environments where regular features like orthogonal and parallel line segments and conjugate least-squares surfaces are determined easily [9].

Generally, the forest environment is highly complex and irregular than the urban and indoor environments and shows regular and similar features as in urban and indoor environments. It is absent or difficult to find it [10]. Usually, point-based approaches like ICP require regular detection and ranging points for registering coarsely before executing the algorithm. Moreover, these coarse registrations over the forest environments are generally attained by manual selection of tie points which is time-consuming and labor-intensive.

In recent times, there are diverse marker-free data-based fusion approaches anticipated by various researchers to handle the issues in missing reference features over forest regions. For instance, H. Guan et al. [11] uses geometrics features over the light-based detection and ranging points for registering the multi-scale TLS data. H. Song et al.[12] anticipated a multi-scan data registration approaches with the adoption of populated triple sets, eigenvalues, and tree locations. X. Liu et al. [13] adopt simulated annealing to predict the optimal 3D-transformation among the corresponding coordinate systems of the tree locations derived from the UAV and backpack data. These approaches rely entirely on the geometric information of tree-stem, or it looks for the globally optimized registration outcomes with tree attribute constraints like tree locations and DBHs. Moreover, the geometric information of tree steam is generally not available from the top-end data like UAV data and optimized globally to attain a solution that fails in accuracy estimation of tree-related attributes, and the accuracy is generally lower. The major challenge of this study is how to efficiently and accurately register the multi-

platform points in the forest regions? And how is this challenge efficiently handled for forest applications? H. Xia et al. [14] discuss a novel multi-platform data registration framework for forest applications using the unique spatial tree distribution over the forest regions by registration process [15].

2. RELATED WORKS

Drylands face crucial challenges with native vegetation deterioration due to anthropogenic activities and climatic changes, as Nogueria et al. [16] described. These activities are crucially influenced by the ecosystem's available services and vegetation patterns, and it causes harmful influence over the natural resources and human-being sustainability. Dryland ecosystems are characterized by constraint and sparse native vegetation due to weather conditions, i.e., low precipitation and high temperature. Moreover, vegetation in the desert region plays a substantial role in battling promulgating carbon sequestration. Guo et al. [17] discuss the significance of native vegetation, which is crucial for understanding the atmosphere and earth, like soil erosion, droughts, and climatic changes. Therefore, monitoring vegetation is a pre-dominant phase in restoration to identify degraded fields. Zou et al. [18] discuss the concepts of remote sensing images for the past few decades and offer synoptic insight towards the territory coverage and hauling out essential information on the phenomenon with nominal economic factors. These technologies provide information extraction from the ecological elements merged with the ancillary data over the GIS to evaluate degradation over a certain period. Thus, researchers use spectral measurements acquired from various satellite sensors like vegetation indices (VI) to examine the seasonal vegetation and compute the drought consequences.

Various investigators perform extensive studies on remote sensing to monitor and map vegetation at regional and local scaling based on the different sensors discussed by [19]. The sensors acquire the images in pre-defined spatial resolution to specify ground measurement [22]. Spectral resolutions change due to wavelength intervals as sensors collect the earth's surface reflectance. The temporal resolution of the provided remote sensing images is attained from the speed and orbital path. It shows the satellite revisit rate for gathering ideas from a specific location [23].

3. METHODOLOGY

This section shows three stages for predicting the growth of trees over the drylands. It includes dataset acquisition, segmentation, and classification. Here, the deep learning classifier model plays a substantial role in the prediction process. The simulation is done in the MATLAB 2018a environment, and metrics like prediction accuracy are evaluated to show the significance of the model.

a. Dataset

Here, Moderate Resolution Imaging Spectroradiometer (MODIS) is used for monitoring the development and vegetation growth over the land covers of Tamil Nadu (TN). MODIS is available for a 500m resolution (8 days) temporal period to derive the Normalized Difference Vegetation Index (NDVI) for mapping the terrestrial

vegetation. The onboard terra sensor surface was downloaded from (HTTP:// search.earthdata.nasa.gov). It is mathematically expressed as in Eq. (1):

$$NDVI= (\rho (NIR-red))/(\rho (NIR+red)) \quad (1)$$

Based on Eq. (1), the theoretical values are specified based on the ratio ranging from -1 to +1; however, the higher IV is related to higher biomass where the index value (bare soil, water bodies, and non-vegetated areas) falls nearer to 0. Table 1 depicts the various land cover regions of TN and corresponding geographical regions. Table 2 depicts the NDVI during vegetation greening and browning.

Table 1 Land covers of TN and geographical regions

S. No	Coverage region	Area (sq.km)
1	Built-up	5289.639
2	Cropland (Rabi)	13630.053
3	Cropland (Kharif)	5232.519
4	Forest (Scrub)	2559.802
5	Forest (Swamp)	166.526
6	Forest (Evergreen)	5434.105
7	Forest (Deciduous)	8684.933
8	Plantation region	9070.512
9	Wasteland	536.470
10	Water bodies	8310.207
11	Wetland	950.959

Table 2 Natural vegetation (pixel %)

	NDVI	
Season	**Positive (%)**	**Negative (%)**
Rabi	59.73	40.29
Kharif	86.53	13.49

b. Traditional Convolutional Neural Networks (CNN)

The most commonly known and notable network model provides superior performance for learning features and performs classification. It is an FFNN (Feed Forward Neural Networks), and the parameters are trained with conventional stochastic gradient descent. The CNN model comprises various blocks known as convolutional, pooling, and fully connected (FC) layers. These processing layers play a substantial role in the

network model. The former convolutional layer carries out convolution operations among the input, filters, and output feature maps. Generally, feature mapping is performed in a non-linear activation function (AF). The non-linear transformation is done in Rectified Linear Unit (ReLU) for feature mapping generated by the first convolution layer. It initiates system non-linearity and is used for AF. The convolution layer functionality is to haul out various input layered features and attain weight sharing. Every stage's input/output features are provided in a set of array forms and known as feature maps. For instance, if the 2D input images x, the provided input is decomposed in a sequential manner x={x_1,x_2,…,x_3}. The convolutional layers are expressed as in Eq. (3):

$$y_j = f\left(b_j + \sum_i k_{ij} * x_i\right)$$

Here, y_j specifies the j^th output of the convolutional layer, and x_i specifies the input feature map, k_ij is the convolutional kernel with input map x_i. * specifies discrete convolutional operator, f is non-linear activation function, b_j is trainable bias. The pooling layers perform the sub-sampling function to diminish the feature mapping dimensionality. Based on the average and maximal functions, the functionality of the pooling layer is partitioned as average and maximal pooling. The fully connected layers are known as FFNN, which performs higher-level feature abstraction. Often, it is the last layer and performs the final non-linear feature combination to perform the prediction process. The activation functions of the FC layer have to be chosen with practical tasks. The sigmoid functions or softmax are adopted for evaluating the posterior probability of the grid.

c. Regional Convolutional Neural Networks (R-CNN)

The architecture of the proposed R-CNN model is performed using the AlexNet model. The anticipated R-CNN model and the hyperparameters are tuned based on the dataset. The input patches are provided as a 3D data representation of a*a*z with 25*25*11. The regional CNN model is composed of 3 convolution layers, two pooling, and 3 FC layers. Convolution layers have 64, 128, and 256 kernels and 256 kernels with 3*3 uniform kernel sizes. The convolution layers are followed by ReLU activation functions and the pooling layer. Here, zero padding is used for retaining the dimensionality, and the pooling layers perform maximal pooling. Zero padding is used for retaining the dimensionality, and the pooling layer performs maximal pooling and summarizes 2*2 neighborhoods with 2-pixel strides.

The three weighted layers are FC layers with 128, 64, and 32 neurons. The FC layers output is fed to a 2-way classifier known as softmax and evaluates the probabilities of the class labels. The CNN parameters are learned automatically during training and represented as the convolutional layers' kernel and FC layers' weight. R-CNN training is performed to predict the suitable parameters to reduce the error among the ground truth labels and predicted results on the training dataset. Here, the anticipated R-CNN model converts the input patches from the pixel values to the probability classification outcomes. Figure depicts the flow diagram of the anticipated R-CNN model.

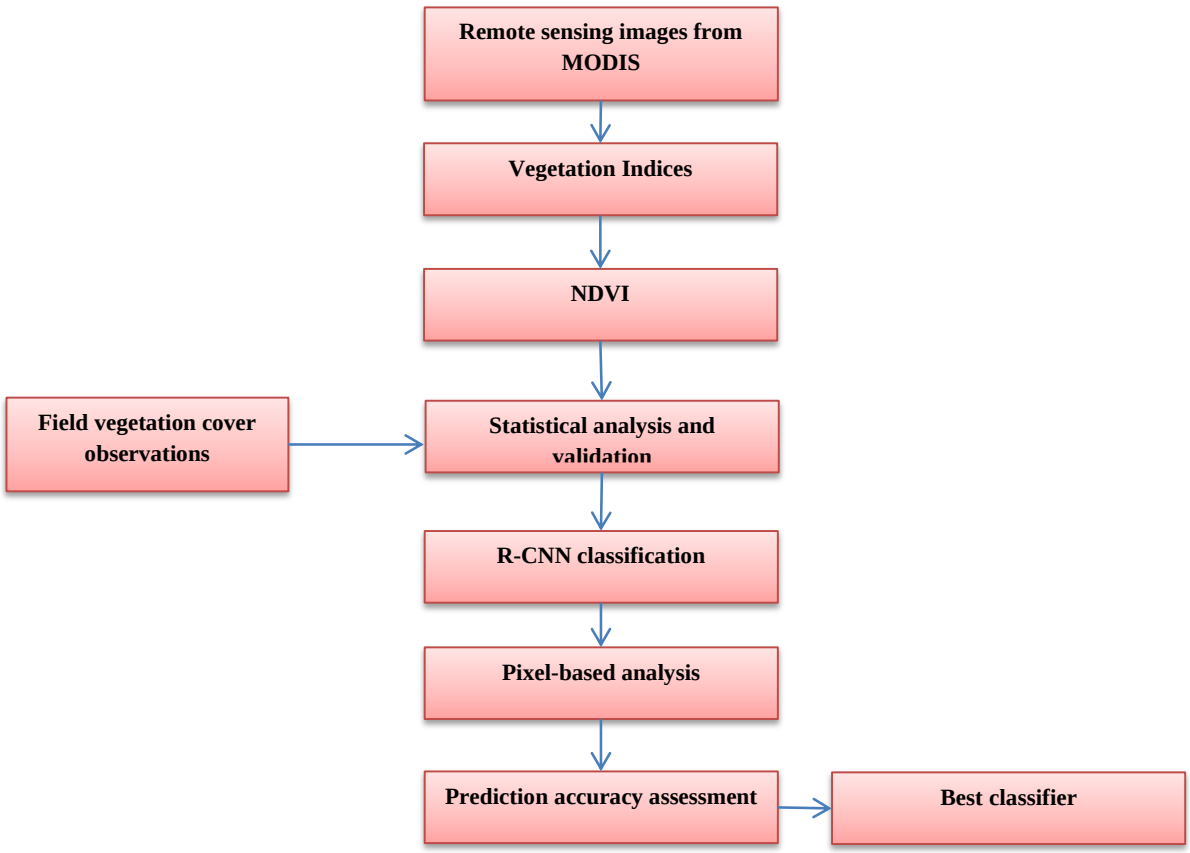

Figure 1: Flow diagram of the R-CNN classification model

The parameters are evaluated using the loss function via FFNN. The learning parameters are updated based on the loss value using the stochastic gradient. The hyper-parameter variables need to be provided for initiating the training process. Recently, dropouts are commenced with a regularization approach, and dropout rates do FC layers, and the value is set 0.5 to reduce over-fitting. Random search is more efficient for hyper-parameter optimization than manual and grid search. The random search was adapted to hyper-parameter optimization and enhanced the speed and accuracy of the model. Table 5 depicts the R-CNN hyper-parameter values.

Table 3: R-CNN parameters and hyper-parameters

	Parameters	**Hyper-parameters**
Convolutional layer	Kernels	Kernel size: 3*3; No. of kernels 64, 128, 256,Stride = 1 Padding, AF = ReLU
Pooling layer	---	Pooling, Max_pooling, Filter size 2*2, Stride 2
FC layer	Weights	AF: softmax, No. of weights
Other		Weight initialization , Optimizer, Loss function Window size, Epochs, Dropouts, Learning rate

The R-CNN model is appropriate for vegetation analysis, and it cannot reveal more information than the available data. The predominant benefit of CNN relies on how this spatial information is extracted with the model.

4. NUMERICAL RESULTS AND DISCUSSIONS

This section discusses the numerical outcomes of the proposed R-CNN model. The simulation is done in MATLAB 2018a environment on Intel Core i5 processor, Windows 8 OS, and 16 GB RAM. Some of the evaluation criteria are considered the key factor for evaluating the classification performance and guide the classifier model to provide better prediction accuracy. There are five statistical measures like overall prediction accuracy; sensitivity, specificity, negative predictive value (NPV), and positive predictive value (PPV) improve classification ability. These metrics are mathematically expressed as in Eq. (4) – Eq. (7):

$$Accuracy = \frac{TP + TN}{TP + TN + FP + FN} \quad (4)$$

$$Specificity = \frac{TN}{FP + TN} \quad (5)$$

$$Sensitivity = \frac{TP}{TP + FN} \quad (6)$$

$$PPV = \frac{TP}{FP + TP} \quad (7)$$

$$NPV = \frac{TN}{FN + TN} \quad (8)$$

Here, True Positive (TP) and True Negative (TN) is depicted as the number of samples classified appropriately as positive and negative samples, respectively. False Positive (FP) and False Negative (FN) are the numbers of misclassified samples. Sensitivity is depicted as the percentage of positive samples appropriately classified, and specificity is defined as the percentage of negative samples adequately predicted.

Table 4: Comparison of various metrics during the training process

Phase	Performance	R-CNN	CNN	RF	SVM	MLP	KLR
Training	**TP**	3127	3127	3054	2861	2800	2940
	TN	2997	2997	2797	2323	2350	2372
	FP	199	200	400	875	850	823
	FN	65	70	143	340	396	345
	Sensitivity (%)	98.58	97.85	95.57	89.60	87.65	89.6
	Specificity (%)	94.50	93.78	87.52	72.70	73.53	74.25
	PPV	98.89	94.03	88.45	76.70	76.9	78.15
	NPV	96.58	97.76	95.18	87.40	85.8	87.5
	Overall prediction accuracy (%)	**96.58**	95.85	91.60	81.5	80.60	81.99

Table 5: Comparison of various metrics during the validation process

Phase	Performance	R-CNN	CNN	RF	SVM	MLP	KLR
Validation	**TP**	740	740	582	533	492	580
	TN	667	667	770	750	764	722
	FP	130	134	32	53	37	78
	FN	60	61	220	270	310	223
	Sensitivity (%)	93.56	92.50	72.60	66.60	62.50	72.25
	Specificity (%)	84.56	83.40	96.15	93.50	95.50	90.25
	PPV	85.86	84.80	94.95	91.2	93.20	88.10
	NPV	82.5	91.75	77.85	73.80	71.25	76.50
	Overall prediction accuracy (%)	90.5	87.95	84.78	80.10	78.50	81.25

The validation phase is utilized to examine the classification performance after every epoch. The validation outcomes are being used whether the training is terminated and hyper-parameters are fine-tuned. The accuracy and loss are two various indicators for computing the training effect. After the training process, the overall prediction accuracy is 96.58%, and the loss is tended to be 0.3 after the 100th epoch. The over-fitting issues are intended to be reduced, and the overall prediction accuracy is 90.5% after the validation process, and the loss is 0.40, respectively. The reduced validation loss specifies that the proposed R-CNN model is aware of over-fitting issues.

Table 6: Comparison of hyper-parameters of benchmark approaches

Approaches	Hyper-parameters
RF	No. of trees = 160, Maximal_features: sqrt, Bootstrap: True, Maximal_depth = 20
SVM	Penalty factor = 100, Kernel function = RBF, Gamma = 1
MLP	No. of hidden layers = 1, Learning rate = 0.001, Momentum = 0.2, Alpha = 0.01, Iteration = 300, Activation function = ReLU, Optimizer = Adam
KLR	Kernel function = RBF, Tuning parameter = 0.02, Regularize parameter = 0.025

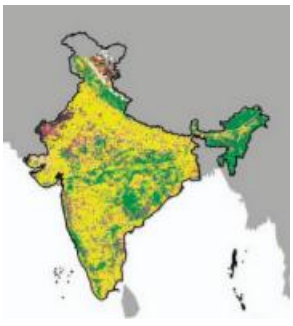

Figure 7. a: Sample 1

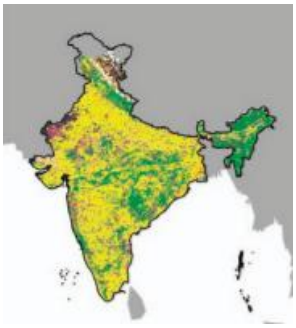

7. b: Sample 2

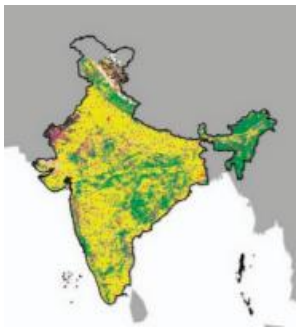

7. c: Sample 3

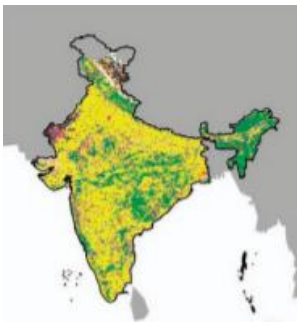

Figure: 7. d: Sample 4

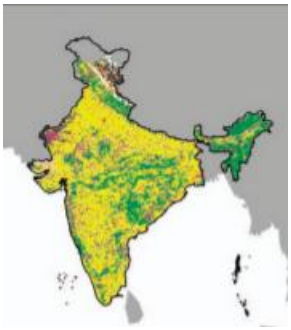

7. e: Sample 5

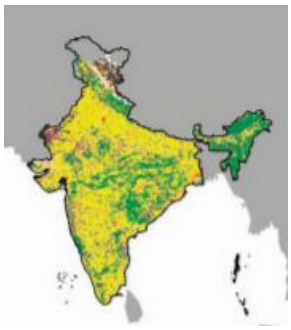

7. f: Sample 6

5. CONCLUSION

In this research, a novel R-CNN model is designed to predict land cover regions using the MODIS dataset. Here, the pre-processing model is explored for predicting the land cover regions to measure vegetative regions. This method is used for predicting the validation and training of the samples. The R-CNN model is more appropriate for the prediction of land cover susceptibility. Hyper-parameters are optimized to enhance prediction accuracy. Various common approaches consider regularization, training samples, architecture complexity, and batch normalization are utilized in the R-CNN to reduce overfitting and underfitting issues. The dataset is fed to the classifier model, and the prediction probability was designed. Finally, the R-CNN performance was evaluated with conventional ML approaches using metrics like accuracy, sensitivity, specificity, PPV, and NPV. The sensitivity of R-CNN model is 98.58%, 94.50% specificity, 98.89% PPV, 96.58% NPV, and 96.58% prediction accuracy. However, there are various constraints in this research. For instance, the impact of diverse R-CNN models for predicting outcomes is not evaluated. Additionally, some appropriate data is required for the experimental validation of the approaches. Recently, the R-CNN methods are extensively increasing. Various diverse architecture is derived, and different classifiers models need to be proposed. Exploring and comparing various classifiers is not appropriate to enhance the prediction process in the future.

REFERENCES

1. M. Anderson, J. Norman, W. Kustas, R. Houborg, P. Starks, and N. Agam, "A thermal-based remote sensing technique for routine mapping of land-surface carbon, water, and energy fluxes from field to regional scales," Remote Sens. Environ., vol. 112, no. 12, pp. 4227–4241, Dec. 2008.
2. Xin, P. Olofsson, Z. Zhu, B. Tan, and C. E. Woodcock, “Toward near real-time monitoring of forest disturbance by fusion of MODIS and Landsat data,” Remote Sens. Environ., vol. 135, pp. 234–247, Aug. 2013
3. Piao et al., "Plant phenology and global climate change: Current progress and challenges," Global Change Biol., vol. 25, no. 6, pp. 1922–1940, Jun. 2019.
4. S. Qiu, Z. Zhu, and B. He, “Fmask 4.0: Improved cloud and cloud shadow detection in Landsats 4–8 and Sentinel-2 imagery,” Remote Sens. Environ., vol. 231, Sep. 2019.

5. L. Liu et al., "Mapping cropping intensity in China using time-series Landsat and Sentinel-2 images and Google Earth Engine," Remote Sens. Environ., vol. 239, Mar. 2020.
6. Q. Wang et al., "Fusion of Landsat 8 OLI and Sentinel-2 MSI data," IEEE Trans. Geosci. Remote Sens., vol. 55, no. 7, pp. 3885–3899, Jul. 2017.
7. F. Gao, J. Masek, M. Schwaller, and F. Hall, "On the blending of the Landsat and MODIS surface reflectance: Predicting daily Landsat surface reflectance," IEEE Trans. Geosci. Remote Sens., vol. 44, no. 8, pp. 2207–2218, Aug. 2006.
8. C. M. Gevaert and F. J. García-Haro, "A comparison of STARFM and an unmixing-based algorithm for Landsat and MODIS data fusion," Remote Sens. Environ., vol. 156, pp. 34–44, Jan. 2015.
9. X. Zhu, E. H. Helmer, F. Gao, D. Liu, J. Chen, and M. A. Lefsky, "A flexible spatiotemporal method for fusing satellite images with different resolutions," Remote Sens. Environ., vol. 172, pp. 165–177, Jan. 2016
10. J. Meng, X. Du, and B. Wu, "Generation of high spatial and temporal resolution NDVI and its application in crop biomass estimation," Int. J. Digit. Earth, vol. 6, no. 3, pp. 203–218, May 2013.
11. Sathya, Vignesh Ramamoorthy H, Anticipate Pattern Mining and Temporary Data Features Extraction in Medical Care System - A Study, International Journal of Emerging Technologies and Innovative Research (www.jetir.org), ISSN:2349-5162, Vol.6, Issue 4, page no. pp310-314, April-2019, http://www.jetir.org/papers/JETIR1904A51.pdf.
12. H. Guan, Y. Su, T. Hu, J. Chen, and Q. Guo, "An object-based strategy for improving the accuracy of spatiotemporal satellite imagery fusion for vegetation-mapping applications," Remote Sens., vol. 11, no. 24, p. 2927, Dec. 2019
13. H. Song, Q. Liu, G. Wang, R. Hang, and B. Huang, "Spatiotemporal satellite image fusion using deep convolutional neural networks," IEEE J. Sel. Topics Appl. Earth Observ. Remote Sens., vol. 11, no. 3, pp. 821–829, Mar. 2018.
14. X. Liu, C. Deng, J. Chanussot, D. Hong, and B. Zhao, "StfNet: A two-stream convolutional neural network for spatiotemporal image fusion," IEEE Trans. Geosci. Remote Sens., vol. 57, no. 9, pp. 6552–6564, Sep. 2019.
15. H. Xia, Y. Chen, Y. Zhao, and Z. Chen, "'Regression-then-fusion' or 'fusion-then-regression'? A theoretical analysis for generating high spatiotemporal resolution land surface temperatures," Remote Sens., vol. 10, no. 9, p. 1382, 2018.
16. Y. Sun, X. Zhang, Q. Xin, and J. Huang, "Developing a multi-filter convolutional neural network for semantic segmentation using high-resolution aerial imagery and LiDAR data," ISPRS J. Photogramm. Remote Sens., vol. 143, pp. 3–14, Sep. 2018.
17. Nogueira K, Penatti OAB, Dos Santos JA. Towards better exploiting convolutional neural networks for remote sensing scene classification. Pattern Recogn. 2017;61:539–56

18. Vignesh Ramamoorthy H, Diabetes Forecasting using Modified RBF Neural Networks, International Journal of Scientific Research in Computer Science Applications and Management Studies (IJSRCSAMS), Volume 3, Issue 5, September 2014, ISSN: 2319 – 1953.
19. Guo Y, Liu Y, Georgiou T, Lew MS. A review of semantic segmentation using deep neural networks. Int J Multimedia Information Retrieval. 2018;7:87–93.
20. Zou, X., Cheng, M., Wang, C, Xia, Y., Li, J., 2017. Tree classification in complex forest point clouds based on deep learning. IEEE Geosci. Remote Sens. Lett. 1 (12), 2360–2364. https://doi.org/10.1109/LGRS.2017.2764938 (cit. On pp. 28, 43, 51).
21. Yuan, Q., Wei, Y., Meng, X., Shen, H., Zhang, L., 2018. A Multi-scale and Multidepth Convolutional Neural Network for Remote Sensing Imagery. 11(3), 978–989 (cit. on pp. 50, 55).
22. Zhao, X., Yuan, Y., Song, M., Ding, Y., Lin, F., Liang, D., Zhang, D., 2019. Use of unmanned aerial vehicle imagery and deep learning unit to extract rice lodging. Sensors (Switzerland) 19 (18), 1–13.
23. Zhang, M., Lin, H., Wang, G., Sun, H., Fu, J., 2018. Mapping paddy rice using a Convolutional Neural Network (CNN) with Landsat 8 datasets in the Dongting Lake Area, China. Remote Sens. 10(11).
24. Windrim, L., Bryson, M., 2020. Detection, segmentation, and model fitting of individual trees stems from airborne laser scanning of forests using deep learning. Remote Sens. 12(9). https://doi.org/10. 3390/RS12091469 (cit. on pp. 51, 52).
25. 'Bigdata Analytics: Comparative Study of Tools' published in International Journal of Computer Science (IJCS), Volume 5, Issue 1, No 2, 2017, Page – 995 to 1003, ISSN: 2348-6600 (Impact Factor: 1.357).
26. Weinstein, B.C., Marconi, S., Bohlman, S., Zare, A., White, E., 2019. Individual tree crown detection in RGB imagery using semi-supervised deep learning neural networks. Remote Sens. 11(11), 1–13.
27. Wang, Chen, Cao, An, Chen, Xue, Yun, 2019. Individual rubber tree segmentation based on ground-based LiDAR data and faster R-CNN of deep learning. Forests 10(9), 793.
28. Trier, O.D., Salberg, A.B., Kermit, M., Rudjord, O., Gobakken, T., Naesset, E., Aarsten, D., 2018. Tree species classification in Norway from airborne hyperspectral and airborne laser scanning data. Eur. J. Remote Sens. 51(1), 336–351
29. Sun, Y., Huang, J., Ao, Z., Lao, D., Xin, Q., 2019. Deep learning approaches for mapping tree species diversity in a tropical wetland using airborne LiDAR and high-spatial-resolution remote sensing images. Forests 10(11), 1047.
30. Qian, W., Huang, Y., Liu, Q., Fan, W., Sun, Z., Dong, H., Wan, F., Qiao, X., 2020. UAV and a deep convolutional neural network for monitoring invasive alien plants in the wild. Comput. Electron. Agric. 174 (May), 105519
31. Ronneberger, O., Fischer, P., Brox, T., 2015. U-net: Convolutional networks for biomedical image segmentation. In: International Conference on Medical image computing and computer-assisted intervention, pp. 234–241

32. Riese, F.M., Keller, S., Hinz, S., 2020. Supervised and semi-supervised self-organizing maps for regression and classification focusing on hyperspectral data. Remote Sens. 12(1), 7 (cit. on p. 67).
33. M.Sharmiladevi, Rafion Houdhoyfi and Vignesh Ramamoorthy H, Data Loss Prevention in Detecting and Preventing Data Breaches: An Overview, International Journal of Computer Science and Mobile Applications (IJCSMA), Vol. 8, no. 3, March 2020, pp. 23-31, ISSN: 2321-8363, https://ijcsma.com/publications/march2020/V8I303.pdf.
34. PJ Prajesh, "Monitoring and mapping of seasonal vegetation trend in Tamil Nadu using NDVI and NDWI imagery," Journal of Applied and Natural Science 11(1): 54 - 61 (2019).